DYNAMIC BEHAVIOUR OF BALL BEARING APPLICATIONS WITH CONSTRAINED DAMPING LAYERS

Hedzer G. Tillema
Department of Mechanical Engineering
University of Twente
P.O. Box 217, 7500 AE Enschede
The Netherlands

ABSTRACT

Rolling bearing noise has become an aspect of increasing importance for the performance of rotating machinery, like electric motors and gearboxes. Generally, two aspects are important with regard to bearing noise, i.e. the transmission characteristics and the vibration generation characteristics. A potential source of vibrations are for example manufacturing imperfections of the different bearing components. Damping of bearing vibrations is enhanced by the lubrication film between the rolling elements and the raceway of the bearing. Regarding vibrations of the total application, the reduction of vibration transmission can be increased by applying a constrained viscoelastic layer between the bearing and the housings. To design an effective damping layer a 3D nonlinear time dependent computational model is developed to simulate the dynamic behaviour of a ball bearing application. The bearing model incorporates the stiffness and damping properties of the lubricant. Flexible components including the viscoelastic layer are modelled with FEM and reduced with a Component Mode Synthesis technique. Viscoelasticity is described both in the time and frequency domain by a generalized Maxwell model. The model is validated experimentally using constrained damping layer samples. Results are shown for a typical ball bearing application, showing that a proper design and material selection of the constrained layer is important for the reduction of the overall vibrations of the application.

NOMENCLATURE

$[K]$, $[C]$, $[M]$	stiffness, damping, mass matrix
$[E]$, $[D]$	elastic, viscous material matrix
$[H]$	history matrix
$[N]$	shape functions matrix
$[T_1]$	hydrostatic transformation matrix
$[T_2]$	deviatoric transformation matrix
$[\Psi]$	Modal matrix
$\{\mathcal{H}\}$	history vector
$\{x\}$	generalized coordinates
E	Young's modulus
G_i	shear modulus
G'	storage modulus
G''	loss modulus
K	bulk modulus
R_p	pitch diameter
T	temperature
Z	number of rolling elements
Ω_c	cage rotational speed
δ	contact indentation
ϵ_{kk}	hydrostatic strain
η	loss factor
η_i	dashpot damping coefficient
ζ	reduced time
κ	deflection coefficient
σ_{xy}	stress
τ_i	relaxation time
ω	angular frequency
c	visous damping coefficient
e_{xy}	deviatoric strain
h_0	central film thickness
m_{ir}, m_{or}	mass (inner ring, outer ring)
t	time
u	displacement

1 INTRODUCTION

In the automotive and household appliance industry increasingly higher demands are posed with regard to the acoustical and vibrational performance of rolling bearings. In rotating machinery, like electric motors, the bearings will act both as vibration exciters and as vibration transmitters. The excitation in a bearing is caused by several mechanisms. First, the time dependency of the bearing stiffness as a result of the rotation of the rolling elements causes a so-called *parametric* excitation. Therefore, a geometrically perfect bearing will still generate vibrations. Secondly, small imperfections in the contacting bodies cause vibra-

tions. They are often classified according to wavelength and referred to as waviness. Waviness is caused by irregularities in the manufacturing process like grinding or honing. Finally, surface defects, contamination, grease and the cage contribute to the generation of vibrations in a rolling bearing. Apart from the excitation by the bearing, vibrations can be generated by various other parts in the application. In automotive applications for example gear contacts can cause vibrations. In electric motors electromagnetic forces can be an important source of vibrations. Often, these type of vibrations are transmitted from the rotor or the shaft via the bearings to a housing. In most cases the housing radiates most of the acoustic energy. In this case the rolling bearings act as vibration transmitters. In order to break the transmission path, a soft viscoelastic layer can be applied between the bearing outer ring and the housing. In this way, vibrations of the shaft can be isolated resulting in a reduced noise radiation of the housing. A disadvantage of such a configuration is the decrease in support stiffness of the application. Therefore, a balance needs to be found between vibration isolation and damping on one hand and support stiffness on the other hand. The objective of this study is to develop a tool that can predict the influence of the bearing and the viscoelastic layer on the dynamic behaviour of the application. As a consequence its design can be improved. Therefore, a 3D computational model is presented to simulate the dynamics of a ball bearing application including a viscoelastic layer. First, in section 2, the bearing model is presented. Next, in section 3.1, the equations of motion for a viscoelastic component are derived. It is shown in section 3.2 how experimental material data can be fitted in the frequency domain. A Component Mode Synthesis technique for viscoelastic FEM components is discussed in section 3.3, whereas in section 3.4 some experimental and numerical results are compared. In section 4 the results for a complete bearing application are discussed. Finally, the conclusions are drawn in section 5.

2 BEARING MODEL

2.1 EHL contact model

A rolling bearing is lubricated with oil or grease to reduce friction. The dynamic behaviour of a lubricated ball-raceway contact can be represented by a spring-damper model. Its constitutive behaviour was predicted beforehand by means of transient contact calculations on a single contact[1, 2]. The model assumes a fully flooded oil film between the rolling element and the raceway. In case of an elastohydrodynamically lubricated (EHL) contact the contact force is given by:

$$F_c = \kappa(\delta + h_0)^{\frac{3}{2}} + c(\delta)\dot{\delta} \tag{1}$$

where δ is the contact indentation and h_0 the central oil film thickness[3]. The deflection coefficient κ is determined by the material and geometric properties of the elastic bodies. The viscous damping coefficient $c(\delta)$ is determined by the lubricant properties and the surface velocities in the contact.

2.2 Complete bearing model

A Lagrangian approach is adopted to construct the equations of motion of the different bearing components, i.e. the inner ring and the outer ring. It is assumed that the rolling elements have no degrees of freedom. Therefore, the inner and outer ball-raceway contact together are represented by a single spring-damper model. In that case, the resultant deflection coefficient κ_{res} reads:

$$\kappa_{res} = (\frac{1}{\kappa_i^{2/3}} + \frac{1}{\kappa_o^{2/3}})^{-3/2} \tag{2}$$

where κ_i and κ_o are the deflection coefficients for the inner and outer raceway contact, respectively. The cage is solely accounted for by assuming a constant angle $\Delta\theta$ between two consecutive rolling elements. Except for the local deformations in the lubricated contacts, the outer and inner ring of the bearing are modelled as rigid bodies. Under certain operating conditions the outer ring of a bearing may deform significantly. In that case the outer ring is modelled as a flexible body with the finite element method. The finite element model is reduced with a special Component Mode Synthesis technique (CMS) to reduce computation times. For details the reader is referred to Wensing[1, 4, 5]. The constitutive relations of the EHL contact model are used to describe the interaction between the structural components of the bearing. The equations of motion for the inner ring and the outer ring yield:

$$[m_{ir}]\{\ddot{q}_{ir}\} + \sum_{j=1}^{Z} F_c^j \frac{\partial \delta^j}{\partial \{q_{ir}\}} = \{f_{ir}\} \tag{3}$$

$$[m_{or}]\{\ddot{q}_{or}\} + \sum_{j=1}^{Z} F_c^j \frac{\partial \delta^j}{\partial \{q_{or}\}} = \{f_{or}\} \tag{4}$$

where F_c^j, δ^j, denote the force and indentation of the combined inner and outer ball-raceway contact, respectively. The degrees of freedom for the inner and outer ring are stored in the vectors $\{q_{ir}\}$ and $\{q_{or}\}$. The set of nonlinear equations is solved with the Newmark time integration method in combination with a modified Newton Raphson process.

3 MODELLING OF VISCOELASTICITY

3.1 Time domain model

In order to study transient effects of rolling bearing applications, like for example parametric excitation, the equations of motion need to be derived in the time domain. To be able to predict the influence of a viscoelastic component on this transient behaviour the constitutive relation for linear viscoelasticity and the equations of motion of a viscoelastic component need to be derived as a function of time as well. The convolution integral form is a general constitutive equation for linear viscoelastic material:

$$\sigma(t) = \int_{-\infty}^{t} G_{rel}(t - t')\dot{\varepsilon}(t')\mathrm{d}t' \tag{5}$$

where $G_{rel}(t)$ is the stress relaxation function. In case of a Maxwell representation[6, 7] this function can be written as a series of exponentials reading:

$$G_{rel}(t) = G_0 + \sum_{i=1}^{N} G_i \mathrm{e}^{-\frac{t}{\tau_i}} \tag{6}$$

Here G_0 is the instantaneous modulus of the material whereas G_i and τ_i are the relaxation strenght and relaxation time corresponding to the i-th dissipative mechanism. The time dependence of G_{rel} can be imitated mechanically with a sufficient number of elastic and viscous elements. The generalized Maxwell model consists of a number of parallel joined spring-dashpot systems and a parallel spring (fig.1) for which the relaxation modulus matches equation 6. In general, time dependent behaviour for viscoelastic materials is only present in shear direction[7]. Therefore, the compression stiffness is assumed constant and is defined by a single compression modulus K.

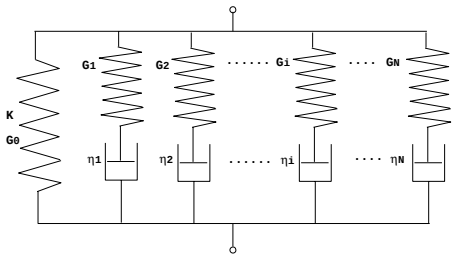

Figure 1: *The generalized Maxwell model*

Advantage of the Maxwell model is that the dynamic behaviour can be described efficiently both in the time and frequency domain. As experimental data for viscoelastic materials are usually given as a function of frequency, it is of great importance that the model can be transformed into the frequency domain in order to obtain the proper material behaviour.

Let us assume a generalized Maxwell model with an additional parallel spring and parallel dashpot. The constitutive equation can then be expressed as:

$$\sigma_{xy}(t) = \frac{1}{3}K\varepsilon_{kk}(t) + 2G_0 e_{xy}(t) + 2\eta_0 \dot{e}_{xy}(t) + \\ + \sum_{i=1}^{N} \int_{-\infty}^{t} 2G_i \exp\left(\frac{t'-t}{\tau_i}\right) \dot{e}_{xy}(t')\mathrm{d}t' \tag{7}$$

where ε_{kk} is the hydrostatic (compressive) strain and e_{xy} denotes the deviatoric (shear) part of the strain vector. The damping coefficient of the parallel dashpot is represented by η_0. The convolution integral represents a sum of the present strain rate and the historical strain rates of the material. For $t < 0$ the material is assumed to be at rest, so the lower boundary of the integral is set to $t = 0$. The convolution integral can be discretized with time step $\Delta t = t^{n+1} - t^n$ according to Baaijens[8]:

$$\sigma_{xy}^{n+1}(t) = \frac{1}{3}K\varepsilon_{kk}^{n+1}(t) + 2G_0 e_{xy}^{n+1}(t) + 2\eta_0 \dot{e}_{xy}^{n+1}(t) + \\ + \sum_{i=1}^{N} \int_{0}^{t^{n+1}} 2G_i \exp\left(\frac{t'-t^{n+1}}{\tau_i}\right) \dot{e}_{xy}(t')\mathrm{d}t' \tag{8}$$

By using the relation $\mathrm{e}^{-t_{n+1}/\tau} = \mathrm{e}^{-\Delta t/\tau}\mathrm{e}^{-t_n/\tau}$ and assuming a piecewise linear rate of deformation $\dot{e}_{xy}$, the integral can be solved and the constitutive equation yields:

$$\sigma_{xy}^{n+1}(t) = \frac{1}{3}K\varepsilon_{kk}^{n+1}(t) + 2G_0 e_{xy}^{n+1}(t) + 2\eta_0 \dot{e}_{xy}^{n+1}(t) + \\ + 2\sum_{i=1}^{N} \hat{\eta}_i \dot{e}_{xy}^{n+1} + \sum_{i=1}^{N} \mathcal{H}_i^{n+1} \tag{9}$$

where

$$\hat{\eta}_i = \tau_i G_i \frac{\Delta t - \tau_i(1 - \mathrm{e}^{-\Delta t/\tau_i})}{\Delta t} \tag{10}$$

$$\mathcal{H}_i^{n+1} = 2\tau_i G_i (1 - \mathrm{e}^{-\Delta t/\tau_i}) \times \\ (1 - \frac{\Delta t - \tau_i(1 - \mathrm{e}^{-\Delta t/\tau_i})}{\Delta t})\dot{e}_{xy}^{n} + \mathrm{e}^{-\Delta t/\tau_i}\mathcal{H}_i^{n} \tag{11}$$

Here the tensor $\mathcal{H}_i^{n+1}$ is the *history* tensor containing the strain rates from the past ($t < t_{n+1}$). Equation 9 is the discretized constitutive equation for a generalized Maxwell model showing the relation between stresses and strains as a function of time. Obviously, a stiffness, damping and history part can be recognized. It should be noted that the equation is written in a convenient, linearized form. Therefore, the computation time is relatively small. Equation 9 is written in matrix notation using the transformation matrices $[T_1]$ and $[T_2]$:

$$\{\sigma\}_{n+1} = [E]\{\varepsilon\}_{n+1} + [D]\{\dot{\varepsilon}\}_{n+1} + \{\mathcal{H}\}_{n+1} \tag{12}$$

where $[E]$ is the elastic material matrix and $[D]$ the viscous material matrix:

$$[E] = K[T_1] + 2G_0[T_2] \qquad [D] = 2(\eta_0 + \sum_{j=1}^{m} \hat{\eta}_j)[T_2] \tag{13}$$

The equations of motion are derived using the procedure of weighting and Galerkin's method. A vector $\{x\}$ is introduced, containing the generalized coordinates. Using a standard finite element approach, Let $[N]$ be a matrix containing the shape functions relating the displacements $\{u\}$ and the generalized coordinates $\{x\}$ and $[B]$ the matrix that relates the strain vector ε with $\{x\}$. The resulting equations of motion for a viscoelastic component yield:

$$[M_{ve}]\{\ddot{x}\}_{n+1} + [C_{ve}]\{\dot{x}\}_{n+1} + [K_{ve}]\{x\}_{n+1} = \{F\} - [H_{ve}]\{h\}_{n+1} \tag{14}$$

where $[M_{ve}]$ is the mass matrix, $[C_{ve}]$ the damping matrix and $[K_{ve}]$ the stiffness matrix of the viscoelastic layer. The vector $\{F\}$ contains the externally applied forces and $[H_{ve}]\{h\}_{n+1}$ the history forces. For convenience $[H_{ve}]$ is called the history matrix:

$$[M_{ve}] = \int_V \rho[N]^T[N]\mathrm{dV} \qquad [\mathrm{C_{ve}}] = \int_{\mathrm{V}} [\mathrm{B}]^{\mathrm{T}}[\mathrm{D}][\mathrm{B}]\mathrm{dV} \tag{15}$$

$$[K_{ve}] = \int_V [B]^T[E][B]\mathrm{dV} \quad [\mathrm{H_{ve}}] = \int_\mathrm{V} [\mathrm{B}]^\mathrm{T}[\mathrm{T_2}][\mathrm{B}]\mathrm{dV} \quad (16)$$

Note that the vector $\{h\}_{n+1}$ corresponds with equation 11, though now expressed in the generalized coordinates $\{x\}$. The equations of motion are solved by means of the Newmark time integration method.

3.2 Frequency domain model

Viscoelastic material data are obtained from a Dynamic Mechanical Analyzer (DMA). This machine measures the stiffness and loss factor of a material for a specific frequency and temperature range. Generally, the working frequency range of the DMA is limited from approximately 0.01 to 200 Hz, whereas the temperature ranges from about -145 to 600 ^0C. In order to determine the shear modulus and accompanying loss factor for a wide frequency range at a certain reference temperature, the time-temperature superposition (TTS) principle is applied[7]. It says that the modulus of a material at time t and temperature T is equivalent to the modulus at the reduced time ζ and a reference temperature T_0. This principle is widely used to extract the material properties over a wide frequency range.

The dynamic shear modulus for viscoelastic materials can be written in complex form, reading:

$$G^*(\omega) = G'(\omega) + jG''(\omega) = G'(\omega)(1 + j\eta(\omega)) \quad (17)$$

where $G'(\omega)$, $G''(\omega)$ and $\eta(\omega)$ denote the materials' storage modulus, loss (or dissipation) modulus and loss factor, respectively. ω denotes the angular frequency. For the generalized Maxwell model with N elements including a parallel spring and dashpot, the storage and loss moduli are given by:

$$G'(\omega) = G_0 + \sum_{i=1}^{N} \frac{(\omega\tau_i)^2}{1+(\omega\tau_i)^2} G_i \quad (18)$$

$$G''(\omega) = \omega\eta_0 + \sum_{i=1}^{N} \frac{\omega\tau_i}{1+(\omega\tau_i)^2} G_i \quad (19)$$

Note that the dissipation modulus of the parallel dashpot is linear with the frequency. Experimental data can be fitted fairly easily using a number of Maxwell elements. In figure 2 the storage modulus and loss factor of a soft rubber are shown. Note that 5 Maxwell elements in combination with a parallel spring and dashpot were used to obtain this result.

For a direct harmonic analysis of a viscoelastically damped structure, the following equation needs to be solved:

$$-\omega^2[M]\{x\} + ([K(\omega)] + j\eta(\omega)[K_{ve}(\omega)]_{dev})\{x\} = \{F\} \quad (20)$$

where $[M]$ and $[K(\omega)]$ are the system mass and frequency dependent stiffness matrix respectively and $[K_{ve}(\omega)]_{dev}$ the deviatoric part of the stiffness matrix of the viscoelastic layer. In this case the material data can be curvefitted by means of a simple exponential function.

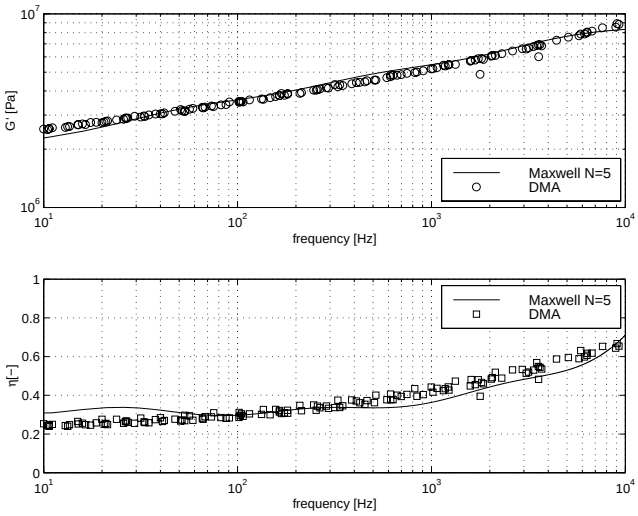

Figure 2: *Maxwell curvefit of the storage modulus and loss factor of a viscoelastic material*

3.3 CMS reduction of viscoelastic components

For an efficient transient analysis of a bearing application, each FEM component in the system, like a shaft or a housing, is reduced individually by means of a Component Mode Synthesis (CMS) technique. In order to deal with complex geometries and complete flexibility for a viscoelastic component one must resort to a finite element approach as well. To enable an easy coupling of adjacent components, the CMS technique must therefore also be applicable to a viscoelastic component. The CMS technique is based on the Ritz method, which describes the displacements of a structure as a series of global shape functions. The number of degrees of freedom of a system can thus be reduced significantly by choosing suitable shape functions in the frequency range of interest. With CMS a set of shape functions or component modes consists of a *static* and a *dynamic* mode set. These modes are required to describe both the static and dynamic solution (and if applicable, rigid body motions) of the structure. The component modes are stored columnwise in the transformation matrix $[\Psi]$. Consequently, the reduced mass and stiffness matrix are obtained by:

$$[m] = [\Psi]^T[M][\Psi] \quad [k] = [\Psi]^T[K][\Psi] \quad (21)$$

The conventional Component Mode Synthesis works most efficient for undamped, slightly damped or proportionally damped systems. In case of a viscoelastic component we assumed damping only in shear direction implying that it is a non-proportionally damped system. However, if the dynamic behaviour of a viscoelastic component can be described efficiently with the use of undamped modes, the reduced matrices can be obtained conform equation 21:

$$[m_{ve}] = [\Psi]^T[M_{ve}][\Psi] \quad [c_{ve}] = [\Psi]^T[C_{ve}][\Psi] \quad (22)$$

$$[k_{ve}] = [\Psi]^T[K_{ve}][\Psi] \quad [h_{ve}] = [\Psi]^T[H_{ve}][\Psi] \quad (23)$$

Note that the reduced history matrix can be obtained because the vector $\{h\}$ is a linear combination of the generalized degrees of freedom. It is clear that the system mass and stiffness matrix can be calculated in a FEM package directly. The system damping and history matrix, however, are not proportional to the mass or stiffness matrix, but proportional to the deviatoric part of the stiffness matrix $[K_{ve}]_{dev}$. Hence, the reduced damping and history matrices can be calculated using equations 13 and 16 in combination with the original set of undamped modes:

$$[c_{ve}] = [\Psi]^T[C_{ve}][\Psi] = \frac{\eta_0 + \sum_{j=1}^{m} \hat{\eta}_j}{G_0}[\Psi]^T[K_{ve}]_{dev}[\Psi] \qquad (24)$$

$$[h_{ve}] = [\Psi]^T[H_{ve}][\Psi] = \frac{1}{2G_0}[\Psi]^T[K_{ve}]_{dev}[\Psi] \qquad (25)$$

In these investigations a viscoelastic layer was considered having a ring shaped geometry with a relatively small wall thickness. The inner and outer surface of the layer are modelled as two rigid interfaces both having 3 translational and 3 rotational degrees of freedom. Therefore, a set of 12 *static* modes is used to reduce the system matrices. As no dynamic effects over the thickness of the layer are expected, the use of *dynamic* modes is considered redundant.

3.4 Experimental verification

Several constrained damping layers were manufactured to verify the viscoelasticity model. The samples consist of two thick concentric (elastic) rings with a highly damped rubber material clamped in between (see figure 3). FRF's were determined by experimental and numerical techniques. The results for three different samples are shown in figure 4.

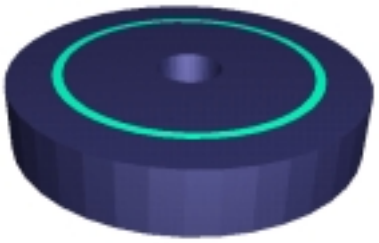

Figure 3: *Constrained damping layer sample*

A good agreement between experiment and prediction can be observed. It should be noted that two highly damped eigenmodes occur around 800 and 1000 Hz. These modes correspond to the rigid body motions of the elastic rings in axial and tilt direction. Due to the high shear rate in the viscoelastic layer a large amount of damping is introduced.

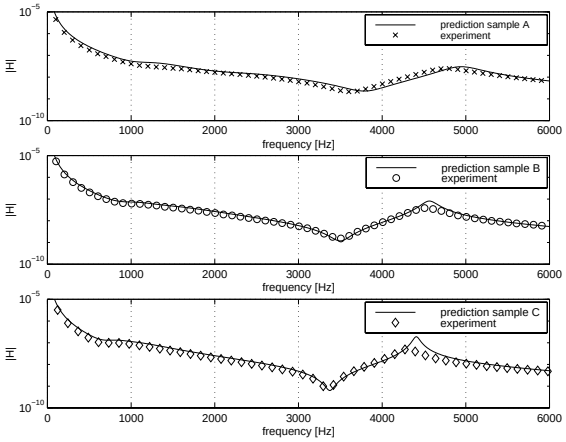

Figure 4: *Calculated and measured FRF's of flexible constrained damping layers*

4 APPLICATION ANALYSIS

In order to study the performance of a viscoelastic layer in a rolling bearing application, a rotor dynamic system containing ball bearings is considered (see figure 5).

Figure 5: *Model of a rotor dynamic application*

The application consists of a flexible shaft supported by two (rigid ring) bearings, which are mounted in flexible housings. Flexible viscoelastic layers are constrained between the bearing outer bore and the housing inner bore, which are modelled as rigid interfaces. Moreover, the inner rings are rigidly connected to the shaft.

4.1 Harmonic analysis

First, a dynamic analysis was performed on the non-rotating system. The system is excited harmonically by a radial force in the middle of the shaft. Such a force could represent the electromagnetic forces in an electric motor or gear contact forces in a gearbox. Furthermore, an axial preload of $180\ N$ is applied on the shaft to ensure contact of each rolling element with the raceway of the bearing. The bearing is given a constant contact damping coefficient of $c = 30\ Ns/m$. The response of the end of the shaft and the top of the housing are exported. A comparison is made between the application without and with viscoelastic layer. Moreover, a variation in the material loss

factor and layer design is investigated. The vertical response function (FRF $H = X_{shaft}/F$) of the shaft is depicted in figure 6:

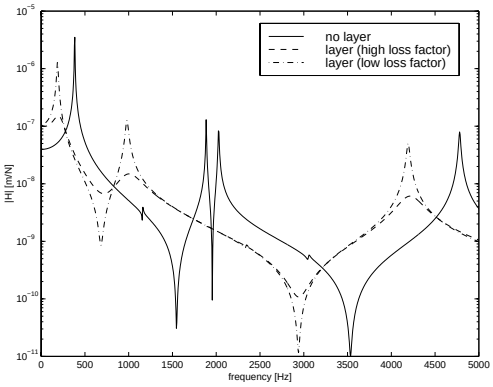

Figure 6: *FRF of the shaft in vertical direction*

In this figure several eigenfrequencies can be distinguished. The peaks at 382 Hz, 1885 Hz, 2027 Hz and 4756 Hz for the application without a damping layer correspond to bending modes of the shaft (figure 7).

Figure 7: *Some important natural modes of the application*

As a result of the reduced stiffness when a viscoelastic layer is added to the system, these eigenfrequencies will shift to lower values . Note that the stiffness reduce is also seen for the zero frequency limit, i.e. the static stiffness in vertical direction. Clearly, the resonance peaks are damped when a viscoelastic layer is applied. The damping increases with a higher material loss factor.

The vertical and axial response of the housing are shown in figures 8 and 9, respectively. It can be observed that the overall response of the housing decreases significantly with the use of a constrained damping layer. Obviously, vibrations of the shaft are isolated from the housing in an effective way. Note that the damping of resonances of the system depends on the materials' loss factor. The level of vibrations for frequencies in between these resonances is also affected by this material property. It is seen that a high loss factor has a negative effect on the isolation capacity of a soft layer. The noise problem in

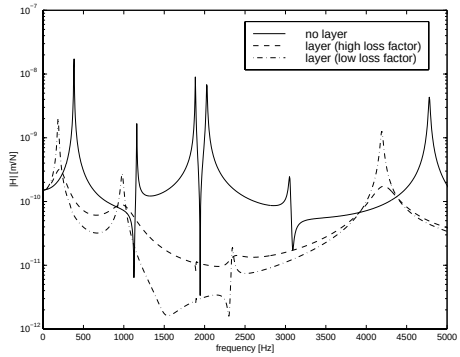

Figure 8: *FRF of the housing in vertical direction*

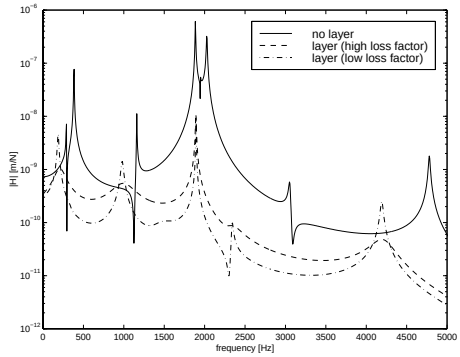

Figure 9: *FRF of the housing in axial direction*

an application, however, is determined mostly by the resonance peaks, i.e. if excited. As these peaks can be reduced more effectively by a high damping material, it is recommended to use such a material. It should be noted that for a proper vibration or noise analysis the consideration of a single response location on the structure is insufficient. It does, however, relate to the dynamic behaviour of the complete system and can therefore give a sufficient indication of the problem area.

4.2 Transient analysis

A rotating case is studied to investigate the effect of parametric excitation. Parametric excitation is caused by the rotation of a finite number of rolling elements over the raceway. As a consequence, vibrations are generated and transmitted through the outer ring. The characteristic frequency of these vibrations is the *ball pass frequency*. This is the frequency at which the rolling elements pass a fixed point on the outer ring, equal to $Z\Omega_C/2\pi$ Hz. Here Z is the number of rolling elements and Ω_C denotes the angular cage velocity. In case of a radial preload on the shaft, the parametrically excited vibrations are enhanced due to the assymetric stiffness distribution in the bearing. Consequently, the rolling elements can lose contact with the raceway and the system becomes strongly nonlinear. For the analysis the

shaft is given a rotational speed of 5000 rpm. An axial preload of $180\ N$ is applied to the shaft. To be able to clearly observe the effects of parametric excitation the shaft was given an additional radial preload of $10\ kN$. A total of 100,000 time steps were calculated, which resulted in a 4 Hz frequency resolution. A calculation was performed of a system without layer and one with a high damping viscoelastic layer. In figure 10 the shaft orbit is shown.

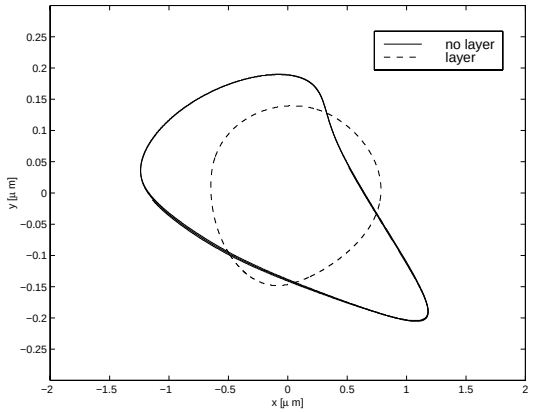

Figure 10: *Shaft orbit*

The frequency in which the shaft makes this orbital motion corresponds to the ball pass frequency. It is seen that the response is not exactly symmetrical about the y-axis due to the rotation of the rolling elements. The response of the shaft for the system with viscoelastic layer is more smooth as the damping in the system has increased. It should be noted that the static deflection in y-direction is substracted from the reponse for clarity.

5 CONCLUSIONS

A threedimensional computational model has been developed to investigate the dynamic behaviour of a rolling bearing application. The bearing model is based on previous research that incorporates lubricant effects and, if necessary, a flexible outer ring.

The constitutive behaviour for linear viscoelasticity was derived in a discretized form. It is based on a generalized Maxwell model in order to facilitate the derivation in both the time and frequency domain. The stiffness and damping properties of a real viscoelastic material can be fitted fairly easily by means of a few Maxwell elements in combination with a parallel spring and dashpot. The equations of motion were derived using a standard finite element approach and are written in a linearized form using the exponentially decaying *history* vector. With this method transient dynamic calculations can be performed relatively fast.

The linear equations of motion for a viscoelastic component allow for the usage of the component mode synthesis. Keypoint in this approach is that the damping and history matrix are proportional to the deviatoric part of the stiffness matrix. The reduction is based on a transformation matrix containing the undamped modes of the system.
The model has been validated succesfully with dynamic experiments.

The analysis of a rotor dynamic application has shown the potential use of a viscoelastic layer with regard to damping and vibration isolation. The harmonic calculation showed a reduction of the response function of the housing when such a layer is applied. The support stiffness, however, also reduced as a result of the relatively soft layer.

The vibration isolation capacity can also be concluded from the velocity spectrum of a rotating, time dependent analysis. The analysis illustrates both the transmission and excitation characteristics of a bearing application.

ACKNOWLEDGEMENTS

The author would like to thank the University of Twente and the SKF Engineering and Research Centre for the support of this project. Especially, the author wishes to thank Dr. J.A. Wensing and Prof. H. Tijdeman for their close cooperation and fruitful discussions.

REFERENCES

[1] **Wijnant, Y.H., Wensing, J.A., Nijen, G.C. van**, *The influence of lubrication on the dynamic behaviour of ball bearings*, Journal of Sound and Vibration, Vol. 222, No. 4, pp. 579-596, 1999.

[2] **Wijnant, Y.H.**, Contact dynamics in the field of elastohydrodynamic lubrication, PhD thesis, University of Twente, Enschede, the Netherlands, 1998.

[3] **Hamrock, B.J., Dowson, D.**, *Isothermal elastohydronamic lubrication of point contacts-Part III*, ASME J. of Lubr. Techn., Vol. 99, No. 2, pp. 264-276,1977.

[4] **Wensing, J.A.**, On the dynamics of ball bearings, PhD thesis, University of Twente, Enschede, the Netherlands, ISBN 90-3651229-8, 1998.

[5] **Wensing, J.A.**, *Dynamic behaviour of ball bearings on vibration test spindles*, 16th International Modal Analysis Conference, Santa Barbara, USA, 1998.

[6] **Alfrey, T.**, Mechanical behaviour of high polymers, Interscience, New York, 1948.

[7] **Ferry, J.D.**, Viscoelastic properties of polymers, John Wiley & Sons, New York, 1980.

[8] **Baaijens, F.P.T.**, Applied computational mechanics, lecture notes, University of Eindhoven, the Netherlands